Proceedings of ICAD2006
4th International Conference on Axiomatic Design
Firenze – June 13-16, 2006
ICAD-2006-26

STOCHASTIC DESIGN IMPROVEMENT OF A STIFFENED FLAT PANEL

Francesco Caputo
francesco.caputo@unina2.it
Seconda Università di Napoli
Via Roma, 29
81031 Aversa (CE)
Italy

Giuseppe Lamanna
giuseppe.lamanna@unina2.it
Seconda Università di Napoli
Via Roma, 29
81031 Aversa (CE)
Italy

Alessandro Soprano
alessandro.soprano@unina2.it
Seconda Università di Napoli
Via Roma, 29
81031 Aversa (CE)
Italy

ABSTRACT

In this work an home-made procedure has been developed, based on the so-called SDI (Stochastic Design Improvement) technique, which is able to perform a preliminary robust design of complex structural components; the procedure is illustrated with reference to the design improvement of a stiffened aeronautical panel, in order to maximize its residual strength in presence of cracks.
The deterministic analyses required to evaluate the influence of the structural parameters have been carried out by means of the finite element method, as implemented in the WARP 3D code; the crack behaviour has been numerically investigated by using the Gurson-Tvergaard model which is enclosed in the library of the same code. Numerical results on the reference component have been validated by using experimental results from literature.

Keywords: R-Curve, Gurson model, SDI, stiffened panel.

1 INTRODUCTION

In recent years structural optimization methods have been increased their relevance in all the main fields of engineering design; the corresponding procedures aim to minimize some functions – following specific routines pertaining to mono- or multi-objective tasks – in presence of prescribed boundary conditions and with reference to the possible range of values where the group of the design variables are defined, while the other possible structural parameters are considered as constant.
Such a design process, however, cannot take into account the scattering of the parameters which randomly influence both the manufacturing process and the service conditions and which, in turn, induce heavy effects on the variability of the performance of the design product.
That consideration clarifies the requirement of a special design methodology, based on probabilistic concepts, as well as complete with procedures and practical tools, such as to make possible to explore in detail the probabilistic aspects involved in the design process of an industrial product in such a way as to obtain a robust design whose behaviour is rather insensitive to all variations of the main variables, or, what is the same, a design whose statistics are characterized by the smallest standard deviation, as a function of the statistics of input.
In the most recent years, in the field of the structural design, the definition of robust design has been subject to a reanalysis, which has resulted in a new design technique called "stochastic design improvement" (SDI).
The initial objective of the reduction of the standard deviation of the output has been replaced by the satisfaction of an assigned condition (target), defined by engineering or marketing considerations, to be reached within an assigned probability value.
In this work an home-made procedure has been developed, based on the SDI (Stochastic Design Improvement) technique, which is able to perform a preliminary robust design of a complex structural component; this procedure is illustrated with reference to the case of a stiffened aeronautical panel, whose residual strength in presence of cracks has to be improved.
The definition of analytical as well as numerical tools to evaluate the residual strength curve (R-curve) of cracked structures is a very interesting task for the scientific community, as it helps to understand some fundamental aspects of the material behaviour to resist fracture.
The approach considered within this work is a micromechanical one, based on continuum mechanics by considering the numerical model as independent from the geometry of considered cracked component, which is able to describe the material behaviour from the starting damaged conditions up to the final collapse.
Ductile fracture begins in many metal alloys with the nucleation of cavities induced by the brittle breaking or decohesion of inclusions.
As these cavities grow in size, they generate local intense stress-strain fields around neighbouring small inclusions, thereby nucleating small-scale cavities which participate to the final phase of the coalescence process and therefore to the macroscopic crack growth. The process of cavity growth is well understood and some models are quite advanced [1 ÷ 3], while the mechanism of nucleation and coalescence, as well as the associated micromechanics, are less well understood.
To develop the study proposed in this work, the deterministic analyses required to investigate the influence of the structural parameters have been carried out by means of the finite element

method, as implemented in the WARP 3D code [4].
The crack behaviour has been numerically investigated by using the micromechanical model of Gurson [5] in the version modified by Tvergaard [6], whose parameters have been determined by using experimental data from metallurgical observations provided from literature [7] and by using a phenomenological fitting home-made procedure which requires combined experimental [8] and numerical simulations.
Numerical results on the reference component have been validated by using experimental results from literature [8].

2 NUMERICAL CALIBRATION OF THE GT MODEL

As it is well known, the Gurson-Tvergaard (GT) model [5 – 6] is represented by the following expression:

$$\phi(q, \sigma_0, f, \sigma_m) = \frac{\sigma^2}{\bar{\sigma}^2} + 2q_1 f \cosh\left(\frac{3q_2\sigma_m}{2\sigma_0}\right) - 1 - q_3 f^2 = 0 \qquad (1)$$

where f is the actual void volume fraction ($f = f_0$ at $t = 0$), σ_m is the hydrostatic pressure, σ is the equivalent Von Mises stress, σ_0 is the yielding stress of the material, q_1, q_2 and q_3 are the Tvergaard correction factors. The void volume fraction rate, df, consists of two terms, df_{growth} and $df_{nucleation}$, respectively linked to the nucleation and the growth of voids. Void coalescence is assumed to start beyond a certain value of f, say f_c, and a macroscopic crack appears when the material ligaments between voids loose completely their capacity to carry a load whatever.
From a numerical point of view, "computational cells", which implements the GT model, are positioned adjacent to the crack propagation plane and are numerically characterized by means of the aforesaid parameters. The numerical characterization of the computational cell, obviously, determines the size of the finite elements used to model the area around the crack tip, by considering one finite element for each cell.
Nine parameters have to be calibrated (by means of a fitting procedure of numerical results with experimental ones) in order to fully characterize the computational cell in the sense above: the three Tvergaard correction parameters (q_1, q_2, q_3); the three parameters associated with the strain normal distribution (mean value, ε_n, standard deviation, S_N, and the volume fraction of void nucleating particles, f_N), which are assumed to govern the strain-induced nucleation rate of voids according to the following expressions:

$$df_{nucleation} = A\left(\overline{\varepsilon_p}\right) d\overline{\varepsilon}_p$$
$$A = \frac{f_N}{S_N\sqrt{2\pi}} \exp\left[-\frac{1}{2}\left(\frac{\overline{\varepsilon}_p - \varepsilon_N}{S_N}\right)^2\right] \qquad (2)$$

where $\overline{\varepsilon_p}$ is the equivalent plastic strain, D_0 is the initial size of the computational cell, f_0 is the initial volume cavity fraction and f_c is its critical value. Another purely numerical parameter, λ, has been considered, which governs the release model for element forces after the void volume fraction reaches the critical value [4].
In fact, at any load step after attaining the critical damage state, the remaining fraction of internal forces applied to nodes of the considered element at crack tip, γ, is given by $\gamma = 1.0 - [(D^* - D_0^*)/\lambda D_0]$, where the D_0^* is the average deformed cell height normal to the crack plane when f is equal to f_c, D^* is the actual deformed cell height and λD_0 represents the allowable elongation of the cell size from the critical condition up to the final cell collapse ($\gamma = 0$), with respect to the undeformed cell height [4].
Beside these parameters it is obviously necessary to know the mechanical properties of the base material (Young modulus, E, Poisson ratio, ν, yielding stress, σ_0, strain hardening, n), or its stress-strain relationship (σ-ε curve). The investigated material has been the aluminium alloy 2024 T3. Standard tensile tests [9] provided the yielding stress $\sigma_0 = 366$ MPa, the ultimate stress $\sigma_u = 482$ MPa and the Young modulus E = 71100 MPa, by which it is possible to calculate the yielding strain $\varepsilon_0 = \sigma_0/E$.
On the base of this data, Tvergaard parameters fitting was performed by comparing two different numerical models under opportune boundary traction [10]; the obtained values are $q_1 = 1.33$;, $q_2 = 0.956$ and $q_3 = 1.77$, confirming the common assumption $q_3 = q_1^2$. In this phase of the fitting process, the nucleation phenomena has not been considered and the f_c value just determines the last point of comparison between the stress-strain curves of the two models without any influence on the fitting process.
The second phase of the GT model parameters calibration process consists in the determination of the nucleation (ε_N, S_N, f_N) and macro-mechanical (D_0, f_0, f_c) parameters. Experimental data related to the considered material are needed to reach this aim, with reference to both a metallographic analysis [7] and an R-curve of the material under examination [8].
For what concerns the metallographic analysis and the defect distribution in the base material it is necessary to assume a first attempt value of the computational cell size, D_0 and of the initial void volume fraction, f_0, to be used in the calibration process.
As it is possible to observe from the data recorded in table I [7], particles or dispersoids are found, which, as it is known, are a cause for void nucleation and therefore can be considered as initial void volume fraction (f_0 = 2.1%). The average distance between the two biggest (> 10 μm) particles is 82.89 μm, which should be approximatively the size of the computational cell.

Equiv Diameter (μm)	Vol Fract (%)	Std Dev	Nearest Neigh. (μm)	Nearest Neigh. Std Dev (μm)	Min. Sep. Dist. (μm)	Min Sep. Dist. Std Dev (μm)	Average size of particles in size category
All Sizes	2,10	0,40	8,58	5,37	5,78	5,30	2,38
1:2	0,18	0,06	15,62	10,78	14,05	11,03	1,46
2:3	0,29	0,07	20,95	13,07	18,27	13,33	2,47
3:4	0,33	0,09	28,23	17,69	24,54	18,17	3,44
4:6	0,49	0,14	26,38	14,85	20,82	15,02	4,85
6:8	0,35	0,15	43,01	25,19	35,00	25,76	6,84
8:10	0,22	0,15	69,60	42,43	59,25	43,54	8,85
10+	0,24	0,24	82,89	54,35	67,90	55,79	12,09

Tab. 1 – Metallographic analysis

With regard to this proposal it must be said that the smaller the computational cell size, the better is the agreement between the experimental and numerical results, but in order to approach the study of complex full scale structures a too small size of the computational cell may constitute a serious problem for what concerns the computational time; therefore, on the basis of the results reported in [11] and of numerical calculations performed by the authors in order to asses those results, a computational cell size D_0 = 200 μm has been considered.

In order to calibrate f_0 and f_c parameters, numerical data have been fitted to experimental ones represented by the R-curve of a central cracked plate under remote traction [8], whose dimensions are 500 mm x 500 mm, with a thickness of 1.28 mm and an initial crack size of 99.6 mm; obtained final values are respectively 0.025 and 0.12. In the same phase of parameters calibration, ε_N, S_N and f_N values have been determined, obtaining $\varepsilon_N = 0.09$, $S_N = 0.045$ and $f_N = 0.11$.

The advantage in the use of such kind of specimen instead of a compact test specimen to characterize experimentally the material toughness is that it provides an easier transferring of the evaluated parameters to the considered full scale components [3], avoiding the difficulties due to the yielding scale at crack tip

3 THE SDI PROCESS: OVERVIEW

A set of techniques has been introduced in order to obtain a robust design, i.e. one whose behavior is rather insensitive to all variations of the main variables, or, what is the same, a design whose statistics are characterized by the smallest standard deviation, as a function of the statistics of input.

This problem can be effectively dealt with by an SDI (Stochastic Design Improvement) [12] process, which is carried out by means of several MC series of trials (runs) as well as through the analysis of the intermediate results.

In fact, input – i.e. design variables **x** – and output – i.e. target **y** – of a mechanical system can be connected by means of a functional relation of the type

$$y = F(x) \tag{3}$$

which in the largest part of the applications cannot be defined analytically, but only ideally deduced because of the its complex nature; in practice, it can be obtained by considering a sample $\mathbf{x}_i$ and examining the response $\mathbf{y}_i$, which can be carried out by a simulation procedure and, first of all, by one of the M-C techniques, as recalled above. Considering a whole set of M-C samples, the output can be expressed by a linearized Taylor expansion centered about the mean values of the control variables, as:

$$y_i = F(\mu_x) + \frac{dF}{dx}(x_i - \mu_x) = \mu_y + G(x_i - \mu_x) \tag{4}$$

where $\boldsymbol{\mu}_i$ represents the vector of mean values of input/output variables and where the gradient matrix **G** can be obtained numerically, carrying out a multivariate regression of **y** on the **x** sets obtained by M-C sampling. If $\mathbf{y}_0$ is the required target, we could find the new $\mathbf{x}_0$ values inverting the relation above, i.e. by

$$x_0 = \mu_x + G^{-1}(y_0 - \mu_y) \tag{5}$$

as we are dealing with probabilities, the real target is the mean value of the output, which we compare with the mean value of the input, and, considering that, as we shall illustrate below, the procedure will evolve by an iterative procedure, it can be stated that the relation above has to be modified as follows, considering the update between the k-th and the (k+1)-th step:

$$\begin{aligned} \mu_{x0} &= \mu_{x,k+1} = \mu_{x,k} + G^{-1}(\mu_{y,k+1} - \mu_{y,k}) = \\ &= \mu_{x,k} + G^{-1}(\mu_{y0} - \mu_{y,k}) \end{aligned} \tag{6}$$

The SDI technique is based on the assumption that the cloud of points corresponding to the results obtained from a set of MC trials can be moved toward a desired position in the N-dimensional space such as to give the desired result (target) and that the amplitude of the required displacement can be forecast through a close analysis of the points which are in the same cloud (Fig. 1): in effects, it is assumed that the shape and size of the cloud don't change greatly if the displacement is small enough; it is therefore immediate to realize that an SDI process is composed by several sets of MC trials (runs) with intermediate estimates of the required displacement (Fig. 2).

It is also clear that the assumption about the invariance of the cloud can be maintained just in order to carry out the multivariate regression which is needed to perform a new step – i.e. the evaluation of the **G** matrix – but that subsequently a new and more correct evaluation of the cloud is needed; in order to save time, the same evaluation can be carried out every *k* steps, but of course, as *k* increases, the step amplitude has to be correspondently decreased.

It is also immediate that the displacement is obtained by changing the statistics of the design variables and in particular by changing their mean (nominal) values, as in the now available version of the method all distributions are assumed to be uniform, in order to avoid the gathering of results around the mode value. It is also pointed out that sometimes the process fails to accomplish its task because of the existing physical limits, but in any case SDI allows to quickly appreciate the feasibility of a specific design, therefore making easier its improvement.

Of course, it may happen that other stochastic variables are present in the problem (the so called background variables): they can be characterized by any type of statistical distribution, but they are not modified during the process.

Therefore, the SDI process is quite different for example from the classical design optimization, where the designer tries to minimize a given objective function with no previous knowledge of the minimum value, at least in the step of the problem formulation.

On the contrary, in the case of the SDI process it is first stated what is the value that the objective function has to reach, i.e. its target value, according to a particular criterion, which can be expressed in terms of maximum displacement, maximum stress, or other.

The SDI process gives information about the possibility to reach the objective within the physical limits of the problem and determines which values the project variables must have in order to get it. In other words, the designer specifies the value that an assigned output variable has to reach and the SDI process determines those values of the project variables which ensure that the objective variable becomes equal, in the mean sense, to the target.
Therefore, according to the requirements of the problem, the user defines a set of variables as control variables, which are then characterized from an uniform statistical distribution (natural variability) within which the procedure can let them vary, observing the corresponding physical (engineering) limits. In the case of a single output variable, the procedure evaluates the Euclidean or Mahalanobis distance of the objective variable from the target after each trial:

$$d_i = \left| y_i - y^* \right| \qquad i = 1,2,\ldots,N \tag{7}$$

where y_i is the value of the objective variable obtained from the i-th iteration, y^* is the target value and N is the number of trials per run.
Then, it is possible to find among the worked trials that one for which the said distance gets the smallest value and subsequently the procedure redefines each project variable according to a new uniform distribution with a mean value equal to that used in such "best" trial.
The limits of natural variability are accordingly moved of the same quantity of the mean in such way as to save the amplitude of the physical variability.
If the target is defined by a set of output variables, the displacement toward the condition where each one has a desired (target) value is carried out considering the distance as expressed by:

$$d_i = \sqrt{\Sigma_k \left(y_{i,k} - y_k^* \right)^2}, \tag{8}$$

where *k* represents the generic output variable.
If the variables are dimensionally different it is advisable to use a normalized expression of the Euclidean distance:

$$d_i = \sqrt{\Sigma \omega_k \left(\delta_{i,k} \right)^2}, \tag{9}$$

where:

$$\delta_{i,k} = \frac{y_{i,k}}{y_k^*} - 1, \qquad \text{if} \quad y_k^* \neq 0$$
$$\delta_{i,k} = y_{i,k} \qquad \text{if} \quad y_k^* = 0 \tag{10}$$

but in this case it is of course essential to assign weight factors ω_k to define the relative importance of each variable.

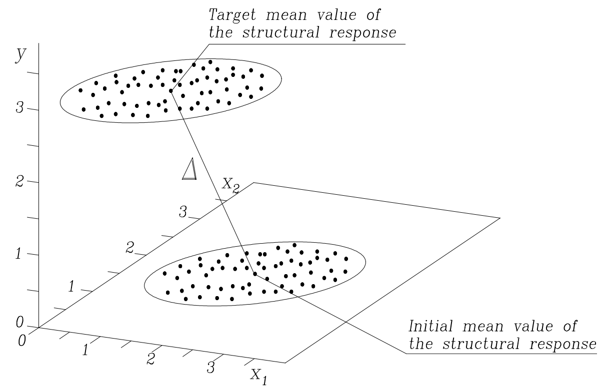

Figure 1 – initial and final structural responses.

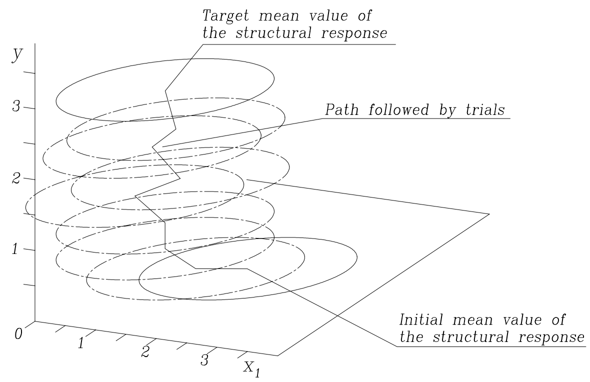

Figure 2 – SDI process.

Several variations of the basic procedures are available; for example, it is possible to define the target by means of a function which implies an equality or an inequality; in the latter case the distance is to be considered null if the inequality is satisfied.
Once the project variables have been redefined a new run is performed and the process restarts up to the completion of the assigned number of shots. It is possible to plan a criterion of arrest in such way as to make the analysis stop when the distance from the target reaches a given value.
In the most cases, it is desirable to control the state of the analysis with a real-time monitoring with the purpose to realize if a satisfactory condition has been obtained.

4 TEST CASE DESCRIPTION

The values obtained through the calibration process discussed in the previous section have been used to evaluate the R-curve of a flat stiffened panel (Fig. 3) constituted by a skin made of Al alloy 2024 T3 LT, divided in three bays by four stiffeners made of Al alloy 7075 T5 L (E = 67000 MPa, σ_y = 525 MPa, σ_u = 579 MPa, δ_{ult} = 16%).

The longitudinal size of the panel is 1830 mm, its transversal width is 1190 mm, the stringer pitch is 340 mm and the nominal thickness is 1.27 mm; the stiffeners are 2.06 mm high and 45 mm width (Fig. 3). The stiffeners were connected to the skin by 4.0 mm diameter rivets (protruding head type), and a continuous rivet pattern was used. Each stiffener was connected to the skin by two rows of rivets in the longitudinal direction.

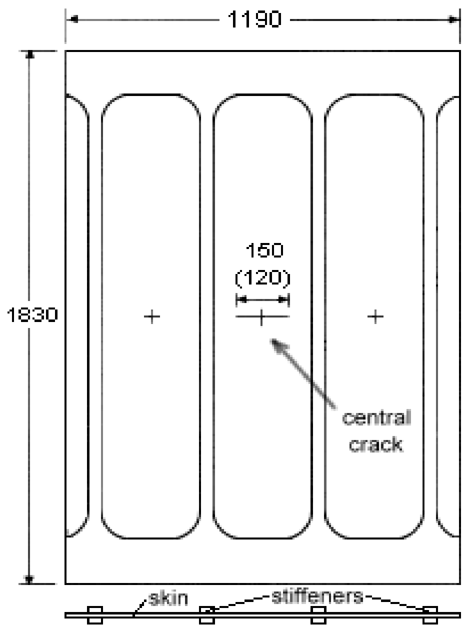

Figure 3 – Stress vs. Crack.

By considering two different panels with just one crack in the middle bay of initial size a_0 respectively equal to 150 and 120 mm, the results reported in figure 4a and 4b have been carried out from both numerical and experimental analyses.

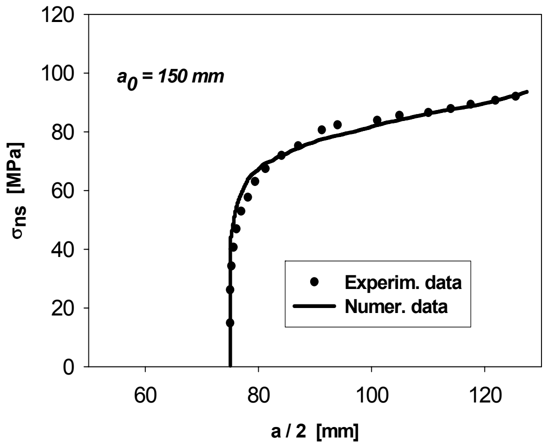

Figure 4a – Panel R-curve.

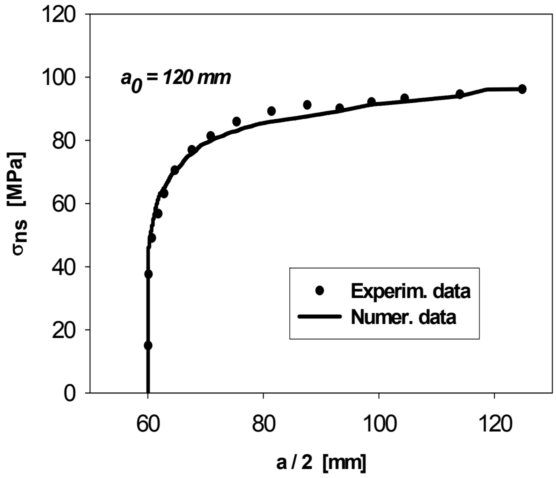

Figure 4b – Panel R-curve

As it is possible to observe, numerical results are in very good agreement with the experimental ones.
In the proposed application of the SDI procedure, a substructure of the panel has been considered, corresponding to a single bay (the part of the panel within the two central stringers) with a fixed width equal to 680 mm, where a central through-crack is assumed to exist, with an initial length of 20 mm.
As design variables they have been considered the pitch between the two stringers and their height.
Their natural variabilities have been considered of ± 10.0 mm for the stringers pitch and of ± 0.4 mm for the stringers height; the engineering intervals of variabilities have instead considered to be respectively [306 ÷374 mm] and [1.03 ÷ 3.09 mm].
An increment of the maximum value of the residual strength curve (Rmax) of the 10 % with a success probability greater than 0.80 has been considered as the target.

5 ANALYSIS OF RESULTS AND CONCLUSIONS

A total of 6 runs, each one of 15 shots have been performed.
It is obvious that at the end of the procedure an extended MC (55 shots) has been performed in order to assess the obtained results from the last run.
In the following figures 5 and 6 the design variables vs. the maximum value of the residual strength has been illustrated.
In correspondence to these two plots we recorded in figure 7 the values assumed by the maximum value of the R-curve for each shot.
In the same figure the reference value (obtained by considering the initial nominal value of the design variables) of the maximum value of the R-curve is reported together with the target value (dashed line).
As it is possible to observe, 9 of the 15 shot of the 5th run overcame the target value; it means that by using the corresponding mean value of the design variable the probability to satisfy the target is of about 0.60.

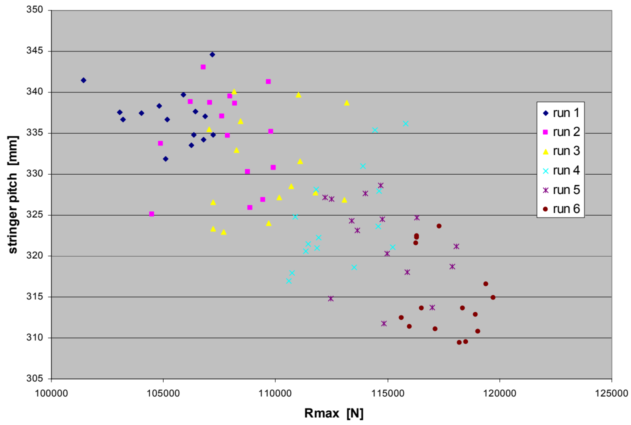

Figure 5 – stringer pitch vs. Rmax.

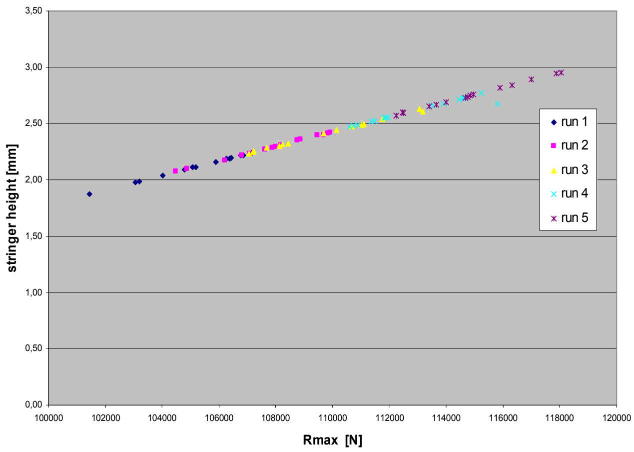

Figure 6 – Stringer height vs. Rmax.

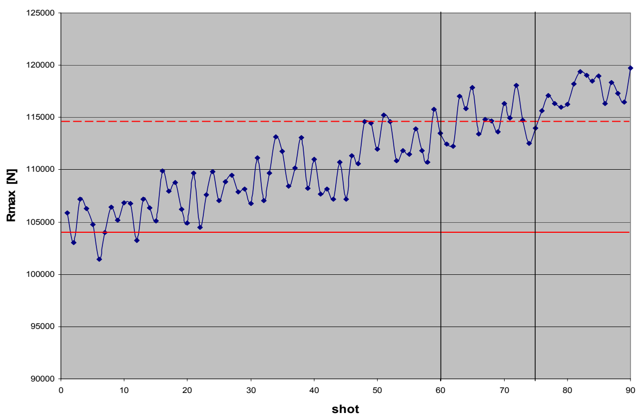

Figure 7 – Rmax vs. shots.

Therefore, another run (the 6th) has been carried out and just one shot doesn't overcome the target value, so that the approximate probability to satisfy the target is about 0.93.

The mean value of the design variables in the 6th run are respectively 318.8 mm for the stringer pitch and 2.89 mm for the stinger height; the mean value of the output variable is 116000 N,.

An extended MC (55 trials) has been performed on the basis of the statistics of the 6th run and the following results have been obtained. In figure 8 the plot of the maximum values of the residual strength for each trial have been reported, while in figure 9 and 10 its mean value and standard deviation vs. the number of the trial have been recorded.

The new mean of the output variable is 117000 N with a standard deviation of 1800 N and the probability to satisfy the target is exactly 0.80.

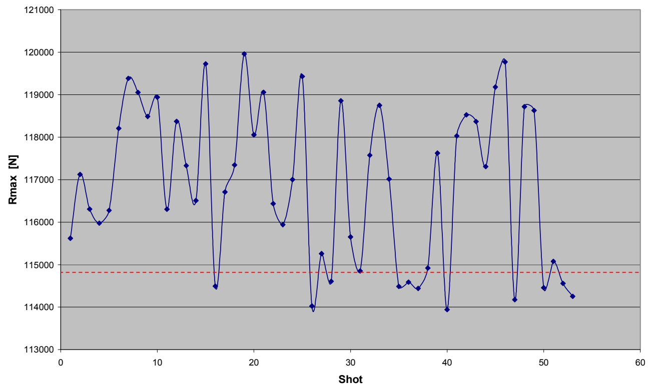

Figure 8 – Rmax vs. shot – extended MC.

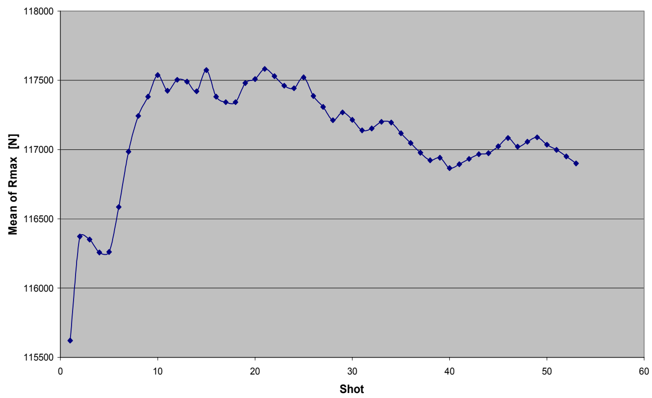

Figure 9 – mean of Rmax vs. shot – extended MC.

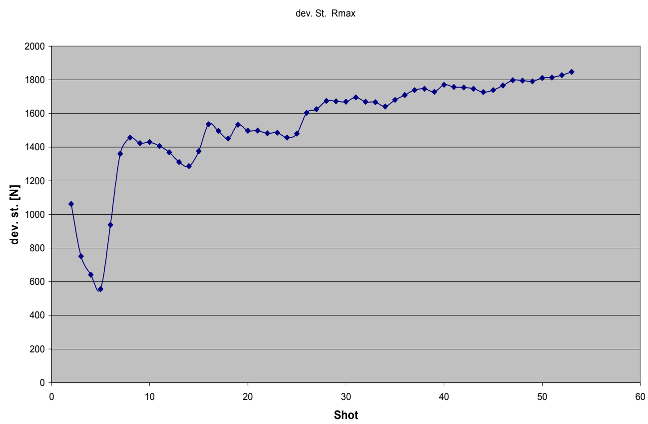

Figure 9 – stddv of Rmax vs. shot – extended MC.

At the end, in the last figure 10, the six R-curves corresponding to the six best shots for each run are reported, together with the reference R-cuve.

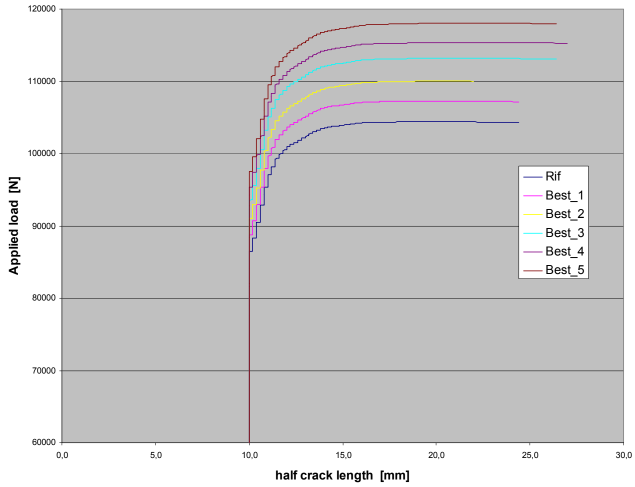

Figure 10 – R-Curves at best shots

6 REFERENCES

[1] R. Mahnken: Int. J. Plasticity Vol. 18 (2002), p. 801.

[2] L. Xia, C. F. Shih, J. W. Hutchinson: J. Mech. Phys. Solids Vol. 43-3 (1995), p. 389.

[3] O. Chabanet, D. Steglich, J. Besson, V. Heitmann, D. Hellmann, W. Brocks: Comp. Mater. Sci. Vol. 26 (2003), p. 1.

[4] A. S. Gullerud, K. C. Koppenhoefer, A. Roy, R. H. Dodds, jr.: *Warp3D- Release 13.8 – 3D Dynamic Nonlinear Fracture analysis of Solids Using Parallel Computers and Workstations*, (University of Illinois, Illinois 2000).

[5] A.L. Gurson: J. Eng. Mater.-T. ASME Vol. 99 (1977), p. 2.

[6] V. Tvergaard: J. Mech. Phys. Solids Vol. 30 (1982), p. 399.

[7] J.S Robinson, *Presentation on the IDA meeting in Geesthacht 22-23 June 2005*, University of Limerick (2005).

[8] H. J. ten Hoeve, L. Schra, A. L. P. J. Michielsen, H. Vlieger, *Residual strength test on stiffened panels with multiple-site damage*, report n: DOT/FAA/AR-98/53, U.S. Department of Transportation (1999).

[8] A. S. Gullerud, K. C. Koppenhoefer, A. Roy, R. H. Dodds, jr.: *Warp3D- Release 13.8 – 3D Dynamic Nonlinear Fracture analysis of Solids Using Parallel Computers and Workstations*, (University of Illinois, Illinois 2000).

[9] *ASTM E-8/69*, Traction Test in Metallic Materials, Annual book of ASTM Standards, vol. 03.01.

[10] J. Faleskog, X. Gao, C. F. Shih: Int. J. Fracture Vol. 89 (1998), p. 355.

[11] D. Steglich, T. Siegmund, W. Brocks: Comp. Mater. Sci. Vol. 16 (1999), p. 404.

[12] I. Doltsinis, F. Rau, M. Werner; Analysis of Random Systems; CIMNE; Edited by I. Doltsinis; Barcelona, Spain; 9-149; 1999.

[13] P. Marek, M. Gustar, T. Anagnos; Simulation-Based Reliability Assessment; CRC Press; Boca Raton, FL; 1995.

[14] R.E. Melchers; Structural Reliability Analysis and Prediction; John Wiley & Sons; Chichester, West Sussex, England; 1999.

